Proceedings of the 28th IEEE
EMBS Annual International Conference
New York City, USA, Aug 30-Sept 3, 2006

Automatic Image Processing Algorithm to Detect Hard Exudates based on Mixture Models

Clara I. Sánchez, Agustín Mayo, María García, María I. López and Roberto Hornero, *Member, IEEE*

***Abstract*—Automatic detection of hard exudates from retinal images is clinically significant. Hard exudates are associated with diabetic retinopathy and have been found to be one of the most prevalent earliest clinical signs of retinopathy. In this study, an automatic method to detect hard exudates is proposed. The algorithm is based on mixture models to dynamically threshold the images in order to separate hard exudates from background. We prospectively assessed the algorithm performance using a database of 20 retinal images with variable color, brightness, and quality. The algorithm obtained a sensitivity of 90.23% and a predictive value of 82.5% using a lesion-based criterion. The image-based classification accuracy is also evaluated obtaining a sensitivity of 100% and a specificity of 90%.**

I. Introduction

DIABETIC retinopathy (DR) is the most common cause of blindness and vision defects in developed countries [1]. Special effort has been undertaken in developing algorithms related to retinal image analysis, providing fundus images enhancement [2], contributing to the monitoring of the disease [3] and developing automatic image analysis algorithms to detect visual signs of DR [4-10], such as hard exudates (HE). HE have been found to be the most specific marker for the presence of co-existent retinal edema, the major cause of visual loss in the non-proliferative forms of DR [1]. Additionally, HE are one of the most prevalent lesions in the early stage of DR [1]. Therefore, the automatic detection of the exudates is useful in a complete automatic analysis of retinal images.

Several investigators have developed techniques for HE detection in fundus images based on a variety of techniques [4-10]. These techniques include image contrast analysis [4-6], Bayesian classifiers [7], [8], and neural networks [9], [10]. Because the brightness, contrast and color of exudates vary a lot among different patients and, therefore, different photographs, these methods would not work in all the images used in clinical environment.

In this study, we have developed a statistical approach based on mixture models to dynamically threshold the images in order to separate HE from background. Mixture models (MMs) have provided a statistical technique for estimating probability densities, such as multimodal histograms [11]. MMs have been used in various applications of medical imaging [12], [13]. Applying MMs, the proposed algorithm achieves a satisfactory detection performance using a dynamic threshold, even on poor contrasted images or with non-illuminated areas.

II. Theory

Let $\boldsymbol{Y}_j$ be a p-dimensional random variable. Assuming that the probability density function $f(\boldsymbol{y}_j)$ can be written as:

$$f(\boldsymbol{y}_j;\boldsymbol{\Psi}) = \sum_{i=1}^{g} \pi_i f_i(\boldsymbol{y}_j;\boldsymbol{\theta}_i) \qquad (1)$$

with $\sum_{i=1}^{g} \pi_i = 1$, it is said that $\boldsymbol{Y}_j$ follows a g-component mixture model (MM) distribution. $\pi_1,...,\pi_g$ are the mixing parameters, $f_1(\cdot),...,f_g(\cdot)$ are the component densities of the mixture, which belong to a known parametric family fully characterized by the parameter vector $\boldsymbol{\theta}_i$, and $\boldsymbol{\Psi} = \left\{\pi_1,...,\pi_{g-1},\boldsymbol{\theta_1}^T,...,\boldsymbol{\theta_g}^T\right\}^T$ is the complete set of parameters needed to specify the mixture [11].

MM is a semi-parametric method suitable for estimating unknown complex probability densities. The standard method to obtain a *maximum likelihood* (ML) estimate of the mixture parameters is the *expectation-maximization* (EM) algorithm [11]. This method is an iterative algorithm which produces the equations for updating the parameters at each iteration step [11].

III. Methods

Let $\boldsymbol{Y}=Y_1,\ldots,Y_n$ be a finite set of pixels from a fundus image characterized by their intensity value Y_j in a color model component. Suppose that a pixel can come from one of the following classes: *class 1* (deep red elements, such as the blood vessels and hemorrhages), *class 2* (background elements) and *class 3* (yellowish elements, such as optic disk (OD), HE and cotton wool spots).

Assuming that the distribution of gray levels for each

Manuscript received 30/03/2006-. This work was partially supported by "Ministerio de Educación y Ciencia" and FEDER grant MTM 2005-08519-C02-01.

C. I. Sánchez is with the Department of Signal Theory and Communications, E.T.S. Ingenieros de Telecomunicación and with the Instituto de Oftalmobiología Aplicada (IOBA), University of Valladolid, 47011, Valladolid, Spain (e-mail: csangut@gmail.com).

A. Mayo is with Department of Statistics and Operative Investigation, Facultad de Ciencias, University of Valladolid, 47005, Valladolid, Spain.

M. García and R. Hornero are with the Department of Signal Theory and Communications, E.T.S. Ingenieros de Telecomunicación, University of Valladolid, 47011, Valladolid, Spain.

M. I. López is with the Instituto de Oftalmobiología Aplicada (IOBA) of the University of Valladolid, 47005, Valladolid, Spain.

class can be modeled by a normal distribution with mean μ_i and variance σ_i, with $i = 1,..,3$, the overall normalized intensity histogram can be written as the following 3-component mixture model distribution [11]:

$$f(y_j) = \sum_{i=1}^{3} \pi_i N(y_j; \mu_i, \sigma_i^2) \quad (2)$$

with $\boldsymbol{\Psi} = \{\pi_1, \pi_2, \boldsymbol{\xi}\}^T$ and $\boldsymbol{\xi} = \left\{\mu_1, \sigma_1^2, \mu_2, \sigma_2^2, \mu_3, \sigma_3^2\right\}^T$.

Our purpose is to identify a significant threshold that allows separating HE from the background. A predefined value cannot be assigned to because the wide variability in the color of fundus from different subjects is strongly correlated to skin pigmentation and iris color. Therefore, we introduce a new approach (Fig. 1) based on mixture models to estimate the image histograms and to obtain a dynamic threshold for each image.

A. Preprocessing

Color normalization and contrast enhancement of the fundus photographs are needed before starting the detection of HE to improve the separation between exudate and non-exudate pixels. A modification of the RGB model is proposed to achieve this aim, obtaining the new color components (R_{mod}, G_{mod}, B_{mod}) as follows:

$$\begin{gathered}(R,G,B) \rightarrow (Y,I,Q) \\ Y_{\text{mod}} = 1.5Y - I - Q \\ (Y_{\text{mod}}, I, Q) \rightarrow (R_{\text{mod}}, G_{\text{mod}}, B_{\text{mod}}).\end{gathered} \quad (3)$$

where (R, G, B) are the three components of the original RGB color model, (Y, I, Q) the components of the YIQ color model and $\rightarrow$ defines the conversion of one color space into another [14]. The resulting image shows an improvement in the overall color saturation and in the contrast between lesions and background (Fig. 2(b)). Moreover, using a quantitative metric to estimate the class separability of exudate and non-exudate pixels in different color models [15], it can be shown that the proposed color model presents the highest metric and its grayscale intensity image (G_R) is the most suitable component for our retinal image analysis.

B. Classification using MMs

Assuming that the normalized intensity histogram of G_R can be modeled as the MM of (2), we apply the EM technique to estimate the mixture parameters. The initialization of the parameters is crucial to the EM algorithm's success because the algorithm's convergence and the final estimate's accuracy depend on these initial parameters [11]. The K-means clustering algorithm is used here to initialize these parameters. This unsupervised technique partitions the dataset into K clusters in order to minimize an objective function, normally the squared error function. This simple algorithm converges fast and allows the initial MM parameters to near optimal values.

C. Thresholding

After the mixture-model parameters have converged, the first Gaussian component is associated with deep-red elements, the second corresponds to the background; and the third component describes yellowish regions. The threshold α_1 is chosen to separate HE from background. It can be set to indicate the percentile of the histogram area defined by the estimated curve that represents *class* 3 (yellow elements). Percentile indicates the percent of the total number of pixels there are in a certain range. This threshold represents an algorithm's parameter. Fig. 2 (c) shows the result with α_1=0.995.

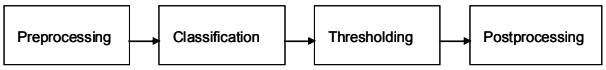

Fig. 1. Block diagram showing the architecture of the proposed image statistical analysis system

D. Postprocessing

After thresholding, other yellow lesions, such as cotton wool spots, the OD and artifacts near the papillary region may be erroneously detected as HE. Therefore, they must be removed from the final result.

In order to mask out the detected OD regions, we have to detect the OD center and its boundary. First, we follow the method proposed in [16] to detect the OD center. This method determined a number of candidate regions with the brightest pixels in intensity image and applied the *Principal Component Analysis* (PCA) based model approach to the candidate regions to give the final location of the OD. We detect the disk boundary using a snake driven by an external field $v(x,y)=[u(x,y),v(x,y)]$ called *Gradient Vector Flow* (GVF) [17] over the image $f(x,y)$.

Cotton wool spots, which present similar attributes to HE but with blurred edges, are removed characterizing the edge strength of the objects in the image. First, edges in the image are enhanced applying the Kirsch's method [14] to the green component of the RGB color model. Thresholding the result at grey level α_2, only the sharpest edges are obtained. This image is combined with the result of the thresholding stage using reconstruction by dilation operation [14] to remove from the final result the elements with high intensity but blurred edges. Fig. 2(d) shows the final result of the detection of hard exudates.

The thresholds α_1 and α_2 are selected as parameters of the proposed algorithm. If they are chosen too low, the sensitivity increases, while the number of false positives may also increase leading to a lower predictivity.

IV. Results

We assessed the performance of our algorithm on retinal images provided by the *Instituto de Oftalmobiología Aplicada* at University of Valladolid, Spain. The images were taken with a TopCon TRC-NW6S Non-Mydriatic Retinal Camera. A total of 10 healthy retinas and 10 fundus images of diabetic subjects with hard exudates were selected to measure the algorithm performance. One specialist performed manual annotations marking HE in all the images.

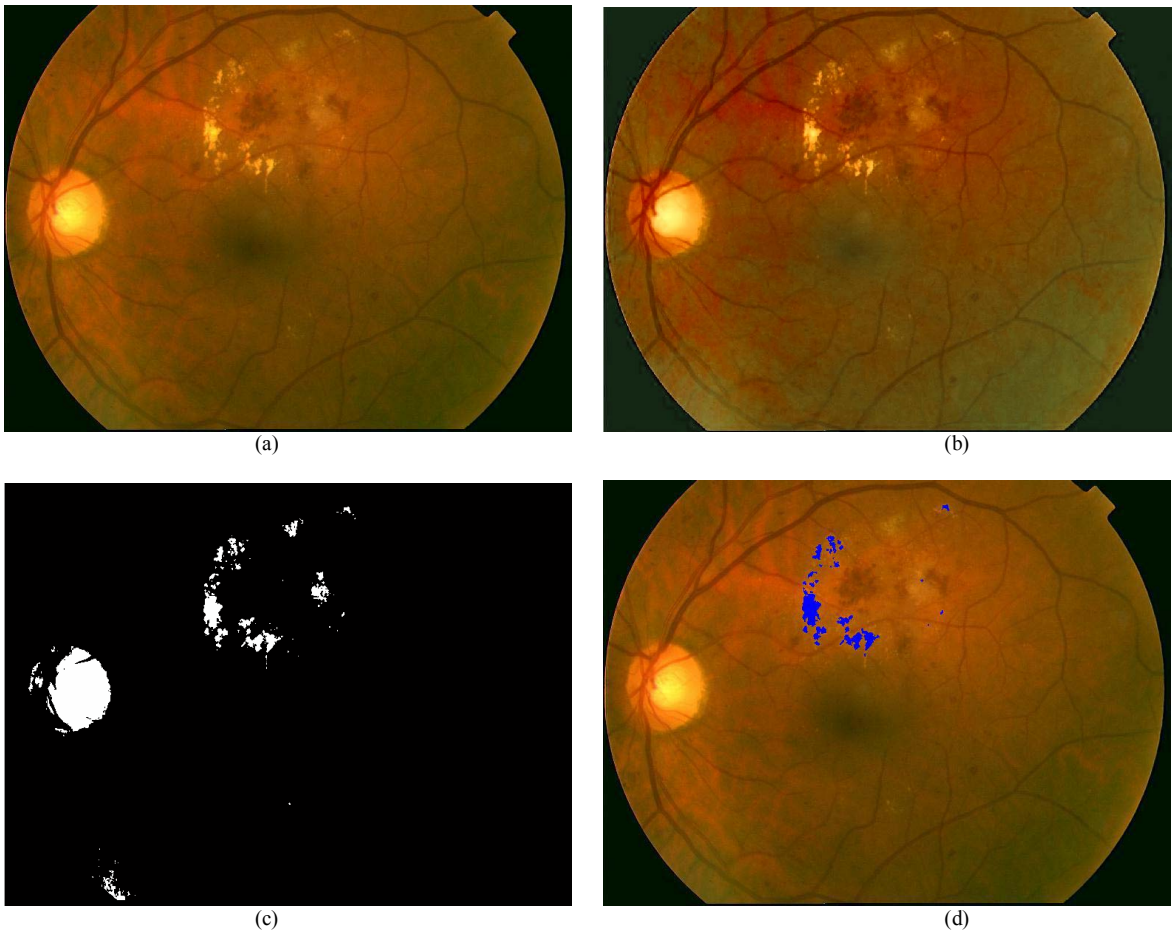

Fig. 2. Detection of hard exudates: (a) original image, (b) image after enhancement, (c) thresholding of yellowish objects, (d) results of the detection of hard exudates.

The algorithm was validated prospectively against expert annotated detection.

In order to assess the algorithm performance in terms of lesion-based criterion and the influence of the parameters α_1 and α_2, the number of true and false positive clusters was firstly determined for each image in the 10 fundus images of diabetic subjects, while the thresholds were varied as follows:

$$\alpha_1 \in \{0.975, 0.99, 0.995\}$$
$$\alpha_2 \in \{0.5, 0.6, 0.7, 0.8, 0.9, 1\} \quad (4)$$

As the number of true negatives (TN) is very high and the specificity measure is not an informative measure in this situation, the ratio TP/(TP+FP), which is the probability that a cluster that has been classified as exudate is really an exudate (predictive value), was used instead. In that way, the sensitivity rate can be plotted as a function of the predictive value, varying the algorithm's parameters [6]. Fig. 3 shows the trade-off between the algorithm's sensitivity and predictivity achieved by inspecting different thresholds. The best performance in terms of lesion-based criterion was achieved at the operation point α_1=0.995 and α_2=0.9 with a sensitivity of 90.23% and a predictive value of 82.5%.

Using this operation point, we evaluated also the algorithm performance to separate images with the presence of exudates from images of healthy retinas. The presence of exudates was successfully detected in all the 10 images from diabetic subjects. In 9 of the 10 images from healthy retinal no exudates were found by our algorithm. In the other image, only a few false positives were found. Therefore, a sensitivity of 100% and a specificity of 90% were obtained in terms of image-based classification accuracy.

V. Discussion and Conclusions

A. Design considerations

The retinal image characteristics have a significant impact on the features of retinal lesions, particularly HE. Consequently, preprocessing techniques are necessary to improve it. Our algorithm obtains color normalization at the same time as contrast enhancement using a particular method for each image: a linear combination of the color bands. This enhancement is independent of external models and only depends on its own intrinsic features, obtaining a dynamic enhancement of the image.

Despite the enhanced appearance of HE, brought about by the preprocessing techniques, their diversity of brightness and size makes it difficult to detect them all. HE usually

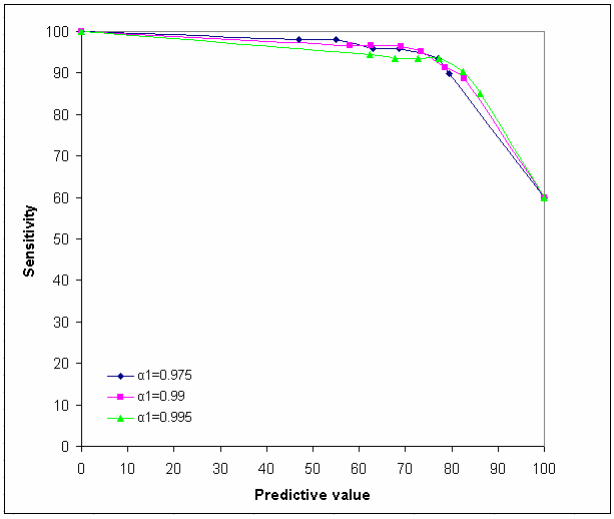

Fig. 3. Sensitivity and predictive value depending on different parameters: $\alpha_1 \in \{0.975, 0.99, 0.995\}$ and $\alpha_2 \in \{0.5, 0.6, 0.7, 0.8, 0.9, 1\}$.

appear in groups and therefore missing some very faint exudates is not very important. However, when there are only a few very faint HE in the retina, the method may fail in the identification task.

We assessed the diagnostic accuracy of our algorithm using a database of healthy retinas and fundus images of diabetic subjects with HE. They showed variable characteristics in terms of brightness, color and contrast to investigate the robustness and the suitability of the algorithm for a clinical environment. Two different criteria have also been used to evaluate the algorithm performance: lesion-based criterion and image-based criterion.

B. Validation databases

Due to the lack of a common database and a reliable way to measure the performance, it is difficult to compare our algorithm to those reported in the literature. Although some works [6], [16], report algorithms with better performance than our algorithm with sensitivities of 92.8% and 100% respectively, the results may not be comparable, since the algorithms were assessed using different databases. In this study, a validation database with manually annotated HE by human experts has been used in order to provide reproducible and comparable performance assessment.

C. Limitations

Using mixture models, we leave out the existence of spatial correlation between observations at neighboring pixels. At the expense of simplicity, structures in form of two-dimensional *Markov Random Field* (MRF) models can be introduced to take into account these local dependences.

The database used to evaluate the method performance is too small to inspire confidence. Therefore, the algorithm should be assessed with more images in order to make the results representative of he clinical problem.

In summary, we developed and validated an automatic detection algorithm for one of the primary signs of DR: hard exudates. This lesion was identified by a dynamic thresholding based on mixture models. After testing prospectively our algorithm with 20 fundus photographs, we have obtained a sensitivity of 90.23% and a predictive value of 82.5% in terms of lesion-based accuracy and a sensitivity of 100% and specificity of 90% using an image-based criterion. Our results demonstrate that the system is well suited to complement the screening of DR helping the ophthalmologists in their daily practice.

REFERENCES

[1] D. E. Singer, D. M. Nathan, H. A. Fogel, and A. P. Schachat, "Screening for diabetic retinopathy," *Ann. Intern. Med.*, vol. 116, no. 8, pp. 660–671, 1992.

[2] M. J. Cree, J. A. Olson, K. C. McHardy, P.F. Sharp, and J. V. Forrester, "The preprocessing of retinal images for the detection of fluorescein leakage," *Phys. Med. Biol.*, vol. 44, no. 1, pp. 293-308, 1999.

[3] A. Pinz, M. Prantl, and P. Datlinger, "Mapping the human retina," *IEEE Trans. Med. Imag.*, vol. 17, no. 4, pp. 606–619, 1998.

[4] N. P. Ward, S. Tomlinson, and C. J. Taylor, "Image analysis of fundus photographs – The detection and measurement of exudates associated with diabetic retinopathy," *Ophthalmol.*, vol. 96, pp. 80–86, 1989.

[5] H. Li and O. Chutatape, "Fundus image features extraction," in *Proc. 22nd Annual Int. Conf. of the IEEE Eng. Med. Biol. Soc.*, 2000, pp. 3071–3073.

[6] T. Walter, J.-C. Klein, P. Massin, and A. Erginay, "A contribution of image processing to the diagnosis of diabetic retinopathy – Detection of exudates in color fundus images of the human retina," *IEEE. Trans. Med. Imag.*, vol. 21, no. 10, pp. 1236–1243, 2002.

[7] K. G. Goh, W. Hsu, M. L. Lee, and H. Wang, "ADRIS: an automatic diabetic retinal image screening system," in *Medical Data Mining and Knowledge Discovery*, K. J. Cios, Ed. New York: Springer-Verlag, 2000, pp. 181–210.

[8] H. Wang, W. Hsu, K. G. Goh, and M. L. Lee, "An effective approach to detect lesions in color retinal images," in *Proc. IEEE Conf. on Comput. Vision and Pattern Recogn.*, 2000, pp. 181–186.

[9] A. Osareh, M. Mirmehdi, B. Thomas, and R. Markham "Classification and localisation of diabetic-related eye disease," in *Proc. of the European Conf. on Comput. Vision*, 2002, pp. 502–516.

[10] G. Gardner, C. Leverton, S. Young, J. Lusty, F. Dunstan, and D. Owens, "Automatic detection of diabetic retinopathy using an artificial neural network: a screening tool," *Br. J. Ophthalmol.*, vol. 80, no. 11, pp. 940–944, 1996.

[11] G. J. McLachlan and D. Peel, *Finite Mixture Distributions*. New York, USA: Wiley, 2000.

[12] I. Frosio, G. Ferrigno, and N. A. Borghese, "Enhancing Digital Cephalic Radiography with Mixture Models and Local Gamma Correction," *IEEE Trans. Med. Imag.*, vol. 25, no. 1, pp. 113-121, 2006.

[13] M. W. Woolrich, T. E. J. Behrens, C. F. Beckmann, and S M. Smith, "Mixture Models with Adaptive Spatial Regularization for Segmentation with an Application to FMRI Data," *IEEE Trans. Med. Imag.*, vol. 24, no. 1, pp. 1-11, 2005.

[14] R. C. Gonzalez and R. E. Woods, *Digital Image Processing*, Reading, MA: Addison-Wesley, 1987.

[15] K. Fukunaga, *Statistical Pattern Recognition*. New York, USA: Academic Press, 1990.

[16] H. Li and O. Chutatape, "Automated feature extraction in color retinal images by a model based approach," *IEEE Trans. Biomed. Eng.*, vol. 51, no. 2, pp. 246–254, 2004.

[17] C. Xu and J. L. Prince, "Snake, shapes and gradient vector flow," *IEEE. Trans. Imag. Process.*, vol. 7, no. 3, pp. 359–369, Mar. 1998.